Nuclear Physics **A352** (1981) 505–534

EQUILIBRATION IN RELATIVISTIC NUCLEAR COLLISIONS. A MONTE CARLO CALCULATION*

J. CUGNON**

W.K. Kellogg Radiation Laboratory, California Institute of Technology, Pasadena, California 91125, USA

T. MIZUTANI

Institut de Physique Nucléaire, Orsay, France

and

J. VANDERMEULEN

Institut de Physique, Université de Liège, Liège, Belgium

Received 4 March 1980
(Revised 2 June 1980)

Abstract: A relativistic Monte Carlo calculation of the nucleus–nucleus interaction in the GeV range is presented. The interaction process is described as a sequence of classical, binary, on-shell baryon-baryon collisions. Pion production is introduced via the formation of Δ-resonances. The latter are given a definite mass and a lifetime against pion emission larger than the collision time. They are, however, assumed to scatter or disappear in collisions with nucleons. At the end of the collision process, they are allowed to decay. The model is used to study the equilibration during a head-on collision between two ^{40}Ca nuclei. The system is found to be compressed up to a time 6–8 fm/c and to decompress very rapidly. The final nucleon and pion momentum distributions are not completely thermalized. They are, however, tentatively described by effective temperatures. The rapidity distributions show larger temperatures than the perpendicular momentum distributions. Also, nucleon temperatures are generally larger than pion temperatures. The theoretical transverse temperatures and the pion multiplicities agree fairly well with the experimental data. The role of the delta particles is investigated. It is shown that the delta production quickens the equilibration process by transforming longitudinal kinetic energy into mass energy. Furthermore, it favours high compression of the system. Non-central collisions are studied. The results are consistent with the concept of geometrical separation between participant and spectator nucleons. However, our model predicts more transparency than the so-called fireball model. The participant part is shown to decompress very rapidly, while the spectator parts are slightly kicked off for intermediate impact parameters. Finally, some results are shown for the case of a head-on collision of a ^{20}Ne projectile by a ^{60}Ni target. A strong shock wave propagates into the target for several fm/c, after which all the matter is dispersed.

1. Introduction

Since its birth a few years ago, relativistic heavy-ion physics has had to deal with some basic questions which have been asked on every occasion: Does the colliding system (at least in a head-on collision) eventually reach some type of thermal equilibrium during a certain period of the collision process? If this is (or is nearly) so,

* Supported in part by the National Science Foundation [PHY76-83685] at Caltech.
** On leave of absence from the Université of Liège, Belgium.

what are the typical temperature and matter density associated with that equilibrium? By merely looking at the inclusive spectra, it would be very difficult to answer these questions as, for example, very different models like the fireball [1]) and the single knock-on [2]) can explain the gross features of the proton cross sections presently available.

In view of the situation mentioned above, we think it worthwhile to study the evolution of a relativistic heavy-ion collision toward equilibrium in a simple, reliable model. In this paper, we report on such a study in the framework of a Monte Carlo model, which simulates the reaction mechanism as a succession of relativistic, binary, classical, on-shell baryon–baryon collisions. A short and preliminary account of this approach has been given previously [3]).

Our Monte Carlo approach incorporates several important aspects: (i) relativistic kinematics is used throughout; (ii) the energy and angular dependence of the elementary nucleon-nucleon cross sections is taken into account; (iii) pion production is assumed to take place in inelastic nucleon-nucleon scattering via the formation of the $\Delta(1232)$ resonance; (iv) the effects of Δ absorption process $N+\Delta \rightarrow N+N$ and elastic Δ–N scattering are taken into account.

We believe the model is suitable for the study of the equilibration process for two reasons. First, there is no assumption about the density or the number of binary collisions, in contrast to many other models. The time variation of these quantities is determined by the dynamics of the model itself. Second, the model has been shown to be very successful in reproducing without any adjustable parameter the inclusive cross sections and the two-proton correlation data at a beam energy of 800 MeV per particle [4]). One has to keep in mind, however, that this success is not strictly a sufficient condition for the appropriateness of the model, as explained above. Rather, the reliability of the model rests on the assumption that the two-baryon collision regime is attained in the energy range we are investigating here. If this assumption is correct, our model is probably the most appropriate description of the relativistic heavy-ion interaction, since this is its basic premise.

Many models have been devised to explain the observable inclusive properties of relativistic heavy-ion collisions. However, only a few investigations have been devoted to the study of the equilibration process: the time evolution of the matter density and of momentum distribution. For the purpose of studying compressional effects, Bondorf *et al.* [5]) developed a model which has some similarity to ours but is more schematic as it neglects inelastic processes. The evolution of the momentum distribution has been investigated first by Hüfner and Knoll [6]) and with refined methods by Knoll and Randrup [7]) in the frame of what is usually called the linear cascade model. At the same time, Randrup [8]) has studied the equilibration in infinite homogeneous nuclear matter. Although the works of refs. [6–8]) are based upon idealized geometrical assumptions, many of their features are confirmed by our calculation. Extensive studies similar to ours have been performed in the framework of the so-called classical equations of motion [9–11]). Our work completes these studies

in the sense that we introduce relativistic kinematics and pion production. Let us also mention, among others, the interesting work of Montvay and Zimányi [12]), who investigate chemical equilibration. Also, several papers have dealt with hydrodynamical calculations of the time evolution of the matter density [13–15]). Although the validity of the hydrodynamical picture can be questioned, they introduce directly the important concept of the nuclear matter equation of state.

Let us finally mention that other three-dimensional cascade codes [16,17]) have been developed. However, they have not been used to study the evolution of the equilibration process [the main differences between these codes and ours is discussed in ref. [4])].

The organization of this work is as follows. In sect. 2 we give a brief description of the model. Sect. 3 is devoted to the study of the head-on collision of two ^{40}Ca nuclei (strictly speaking the collision of two ^{40}Ca-like nuclei since we assume complete isospin degeneracy of the nucleons) at several incident energies. There we follow closely the time evolution of various quantities: baryon density, momentum (rapidity) distribution of baryons and number of Δ-particles. As will be shown, the final rapidity and transverse momentum distributions of both nucleons and pions, are not completely thermal. However, we try to extract some "temperatures" from them in order to characterize them in a simple way. Sect. 4 deals with non-zero impact parameter collision of the same system. We discuss the validity of the concept of spectators–participants separation. In sect. 5 we briefly study the head-on collision of an asymmetric system: ^{20}Ne + ^{60}Ni. Finally, we draw some conclusions in sect. 6.

2. The model

Here, we shall describe briefly the main features of our Monte Carlo calculation.

(i) Initially, the two colliding nuclei are considered as spheres of radius $1.12A^{1/3}$ fm (A: mass number) in their respective rest frames. In each nucleus, constituent nucleons are given their positions and momenta randomly, according to a uniform distribution and the Fermi gas law, respectively, the Fermi momentum being 270 MeV/c.

(ii) For simplicity, we assume the complete isospin degeneracy of the nucleons, making no distinction between protons and neutrons. This applies also to pions and deltas which are discussed below. This assumption is not a very drastic one in view of the nucleon–nucleon scattering properties and the fact that we deal here with self-conjugate nuclei.

(iii) The nuclei are given their initial momenta by Lorentz boosting. Their shapes are accordingly Lorentz contracted.

(iv) The actual calculation begins when these Lorentz contracted spheres touch each other. The scattering process is described by a succession of binary scatterings among the constituent particles. To be more specific, we let all the nucleons move freely (e.g., along straight lines) with their respective momenta until the relative

distance for one of the pairs has reached a minimum. When this minimum distance is smaller than $[\sigma_{\text{tot}}(\sqrt{s})/\pi]^{1/2}$, where σ_{tot} is the total cross section for the pair under consideration at its c.m. energy $\sqrt{s}$, the pair nucleons are allowed to scatter. Once the scattering does take place, whether it is elastic or inelastic is determined randomly according to the relative ratio of the associated cross sections. The momenta of the colliding particles are determined randomly according to the angular distribution of the reaction considered and in a way that conserves energy and momentum (angular momentum is not conserved in this procedure). After the first nucleon–nucleon (N–N) collision has been completed, straight-line motion is resumed and the next possible collision is followed in a similar manner, and so on.

(v) As mentioned in the introduction, inelastic N–N scattering, which is almost entirely dominated by single-pion production in the energy range of our present interest, is assumed to proceed via the formation of the $\Delta(1232)$ resonance, which is assumed to have a definite mass (see discussion of point vii). In other words, we specifically consider the following reactions:

$$\begin{aligned} &\text{(a)}\ \mathrm{N+N\to N+N} \qquad \text{(c)}\ \mathrm{N+\Delta\to N+\Delta} \\ &\text{(b)}\ \mathrm{N+N\to N+\Delta} \qquad \text{(d)}\ \mathrm{N+\Delta\to N+N} \end{aligned} \qquad \text{(e)}\ \mathrm{\Delta+\Delta\to\Delta+\Delta}\,. \tag{2.1}$$

The cross section for reaction (a) is taken from the experimental data. More precisely, we use the curve shown in fig. 1, which is a smooth interpolation of the proton–proton data [18]). Cross section (b) is taken as the inelastic proton–proton cross section. Cross section (d) is obtained from (b) by detailed balance. Cross sections (c) and (e) are not known experimentally, and so have been taken as equal to the cross

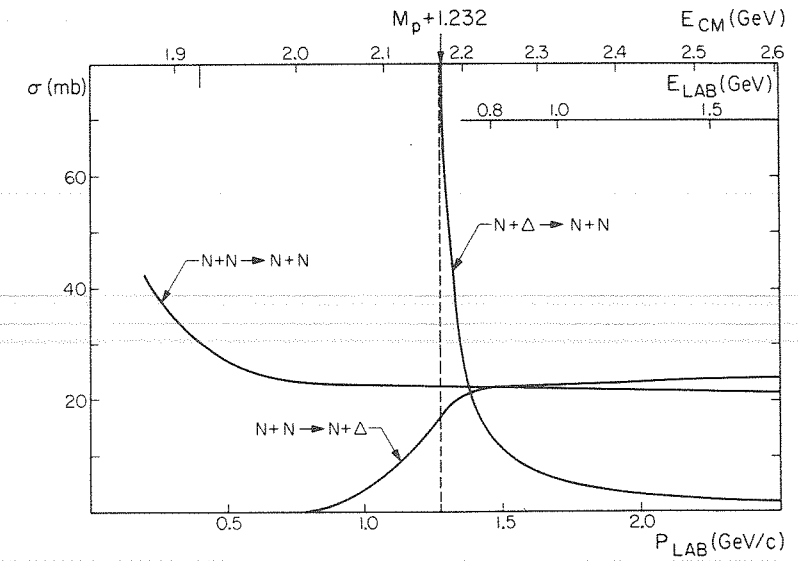

Fig. 1. Cross sections used in the calculation.

section (a) for the same c.m. energy or put equal to zero (see below). For the sake of simplicity, we neglect all the other reactions involving nucleons and Δ-resonances, not listed above. The only one which could play a significant role is $N+\Delta \to \Delta+\Delta$. However, we do not expect its role to be very important below 2 GeV per particle incident kinetic energy in the lab system.

(vi) For the elastically scattered nucleons, the angular distribution is taken as

$$\frac{d\sigma_{el}}{d\Omega} \sim e^{A(s)t}, \tag{2.2}$$

where t is minus the squared momentum transfer and

$$A(s) = 6\frac{[3.65(\sqrt{s}-1.8766)]^6}{1+[3.65(\sqrt{s}-1.8766)]^6}. \tag{2.3}$$

This form, where $\sqrt{s}$ is the c.m. energy in GeV and A is measured in $(\mathrm{GeV}/c)^{-2}$ provides a good fit from $p_{lab} \approx 0.8$ GeV/c, where the cross section is fairly isotropic up to $p_{lab} \approx 4$–5 GeV/c, where it is strongly forward peaked [19]). The same form has been taken for the other elastic cross sections in eq. (2.1). The $N+N \to N+\Delta$ process and its inverse are given an isotropic differential cross section. This choice is due partly to our wish to keep the calculation as simple as possible and partly to our lack of experimental information. However, as a first approximation, this turns out to be all right: for example, a simple calculation of $d\sigma/d\Omega$ ($NN \to N\Delta$) in terms of the lowest-order one-pion exchange contribution [e.g., ref. [20])] (see fig. 2a), which certainly is the dominant contribution [21,22]), gives no eminent maximum or minimum. Also, knowing that this production process at high energies is not dominated by a Pomeron exchange, the forward peaking of this process is not especially favoured. In any event, we investigate below the sensitivity of our results to the Δ-production angular distribution.

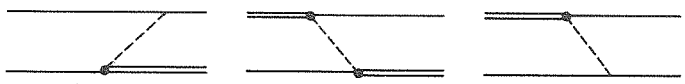

Fig. 2. Elementary diagrams involving Δ-particles.

(vii) Once the delta resonance is introduced to describe the pion production, it is necessary to know its behaviour in nuclear matter, especially at the high densities which may be attained in relativistic heavy-ion collisions. We have already made some brief account of the quantities necessary to characterize the behaviour of the Δ's in ref. [3]), but here we elaborate on it. Rather than comparing various "mean free paths" as in ref. [20]), we would like to look at several partial decay widths, which we think more appropriate since consideration of the Pauli principle is embodied in the so-called Pauli width. We thus base our argument upon the isobar-hole calculation of

the pion-nucleus scattering [23–25]). The most dominant partial width for the Δ is the collision broadening which is due to the exchange scattering by the one-pion exchange (OPE) as shown in fig. 2b. The second dominant one is the width which comes from the Δ-absorption (fig. 2c) by OPE, whereas the Pauli width is smaller than both of these. The value of these widths for nuclear matter densities higher than normal is not well known. But, if the Pauli width is expected to increase with increasing density, the other widths (at least the one associated with fig. 2c) are also expected to do so and the order of dominance could hardly be changed. From the above argument the following may be rather safely concluded. A Δ can decay into a nucleon and a pion, which is predominantly absorbed by another nucleon to form another Δ (fig. 2b) or, alternatively, is absorbed by another nucleon which stays as nucleon (fig. 2c). Thus it is less likely that the pions produced by Δ-decays can escape from the nuclear medium. Taking into account the identity of nucleons, the above picture may be equivalently stated as follows: the produced Δ's mainly undergo elastic scattering with nucleons through OPE interaction of the type in fig. 2b, where the exchanged pion may be real, up until the time when nuclear matter density becomes low enough (in the decompression stage of the heavy-ion collision) at which point the Δ's can all decay freely. In addition to the OPE elastic scattering, some fraction of the Δ's can be absorbed by nucleons through the process $N\Delta \rightarrow NN$.

In view of the above discussion, we have assumed that the Δ's produced by NN collisions survive until the end of the heavy-ion collision process when they decay into N's and π's, and that the Δ-survival is governed by the elastic $N\Delta \rightarrow N\Delta$ and the recombination $N\Delta \rightarrow NN$ cross sections. The end of the collision process is assumed to be reached when the number of baryon–baryon collisions per unit time comes below a certain limit. Most generally, this happens quite abruptly (see below). In the cases studied here, this happens less than 14 to 15 fm/c after the nuclei touch each other.

In our preliminary calculations [3]), we took three different models of the Δ-behaviour: (A) once formed they decay immediately into π and N, and the π escapes from the nuclear medium without interacting, (B) they survive to the end of the collision process with neither elastic $N\Delta$ scattering nor recombination into NN, (C) same as (B) plus elastic scattering of $N\Delta$. Our present discussion seems to rule out model (A). Moreover, in ref. [3]), we show that a short-lived Δ-model can hardly yield the correct π^- multiplicity. In our present study, we improve models (B) and (C) by incorporating the recombination process explicitly. Hence, we will call them models (BR) and (CR) respectively. In order to be consistent with the long lifetime of the Δ, we have taken the inelastic NN cross section to be zero below below $M_p + 1.232$ GeV (see fig. 1).

(viii) The inclusion of relativity in our model calls for some remarks. We have used relativistic kinematics, as is proper at the energies involved. (We have actually carried out some calculations with non-relativistic formulations to find that, for example, the head-on collisions have a tendency to be more explosive.) However, it

is well known that a Lorentz-invariant many-body theory must necessarily be of many-time nature even at the classical level: each particle carries its own proper time. On the other hand, in a conventional cascade calculation, the (three dimensional) variation of spatial distance for every possible pair of particles should be followed to arrange the ordering of binary collisions taking place in cascades (i.e., which pair collides first, which next, etc.). Since the spatial distance separation is not a Lorentz invariant quantity, the time ordering of collisions can be different from one reference frame to another. Although this unpleasant feature may not eventually change the physics, it is inherent to any one-time description. How can we cope with this inconvenience? Consider the spatial distance r_{ab} between nucleons a and b. If the minimum of this quantity has some physical relevance, i.e., some connection with the nature of the mutual interaction (like the interaction radius), it is our physical intuition that its meaning is the most clearly understood in the c.m. frame of particles a and b. In other words, the minimum spatial distance in this frame has to be compared with $(\sigma_{tot}/4\pi)^{1/2}$. Now, r_{ab} transforms into

$$r'^2_{ab} = r^2_{ab} + \gamma^2(\boldsymbol{\beta} \cdot \boldsymbol{r}_{ab})^2 \tag{2.4}$$

in a Lorentz frame moving with velocity β relative to the c.m. frame of a and b. For a relatively high-energy collision, say ≥ 1 GeV/A, the NN collisions which must be considered relativistically are those taking place in the early stages, between nucleons from the projectile and nucleons from the target. The vector minimum distance of approach for such colliding pairs, in the total c.m. frame for instance, is almost perpendicular to the beam direction. This property will be true in any Lorentz frame moving in the beam direction. By virtue of eq. (2.4), the minimum distance of approach is almost invariant in any Lorentz transformation along this direction. Therefore, the dynamics of our calculation is almost invariant under such a Lorentz transformation. We have actually checked this property by calculating collisions both in the total c.m. system and in the target rest frame. Results in one frame when transformed in the other one differ from results directly calculated in the latter by no more than a few percent, in general.

(ix) Quantum effects are neglected. We disregard three-body collisions, the mean field and the Pauli principle (except for what is said in item (x)).

We avoid the introduction of a mean field, because this implies off energy shell scattering, whose cross section is not known and because the explosive nature of the collisions (at least the central ones) very likely destroys the coherence of the mean field soon after the beginning of the process. As a consequence, in our description, the nuclei are expanding, even in the absence of nucleon-nucleon collisions. The expansion is, however, negligible in the short time span during which the strong interaction process takes place [3]).

The effect of the Pauli principle on the nucleons' behaviour is neglected for simplicity. Two important aspects of the high-energy collisions make this procedure reasonable. First, the nucleons have a very large phase space available. Second the

system can be characterized, at the end of the process, by high "temperatures," which reduces the effect of Fermi–Dirac statistics.

(x) Soft nucleon-nucleon collisions are neglected. If the total c.m. energy for a pair of nucleons is less than 1925 MeV, i.e., twice the nucleon mass plus 50 MeV, they are not scattered. This procedure mocks up some Pauli principle effects at the early stages of the process since it partly forbids the collision of two nucleons belonging to the same moving Fermi sphere: 50 MeV is approximately the average of the relative kinetic energy within a typical Fermi sphere. Of course, it also forbids soft collisions between two nucleons, even when the Fermi spheres have disintegrated (say after ~ 8 fm/c, see below). We have, however, checked that the results are not very sensitive to the precise value of the cut-off. This is intuitively understandable for the momentum spectra, since soft collisions are likely to make only small local changes in these spectra.

3. Head-on collision of two $A = 40$ nuclei

The main body of our calculation is devoted to the collision of two ^{40}Ca-like nuclei with zero impact parameter. The results are shown in the total c.m. frame. We have averaged over 40 runs. However, we took advantage of the symmetry to increase the statistics. For instance, the actual spatial matter distribution is symmetric around the collision axis. When described on a three-dimensional grid based upon the three following axes: the collision axis, two axes perpendicular to each other and perpendicular to the first one, it is still symmetric under reflection through any of the planes defined by these axes. A Monte Carlo generated distribution obviously violates somewhat this symmetry. We have symmetrized our calculated distribution, increasing in this way the statistics of the calculation. Typical uncertainties are 7% on the maximum density, 4% on the spectra at their maximum and 5% on the number of Δ-particles.

3.1. DENSITY EVOLUTION

As is well known, the mass density is not a uniquely defined quantity, relativistically. We thus preferred to consider the baryon number density. For this purpose, we have divided the space into cells and counted the number of baryons in each of them at different stages of the collision process. We have studied the baryon number density in the cells in the reaction plane defined by the beam direction (z-axis) and, in this case, any x-axis perpendicular to it. The size of a cell is 1 fm in the z-direction, 0.9 fm in the x-direction and 1 fm in the third direction. In fig. 3a, we show the time evolution of the density profile for the case of model (CR) at beam kinetic energy per particle $E/A = E_{\text{beam}} = 1$ GeV. The first and third columns give the density profile in the z-direction, whereas the second and fourth columns show the profile in the x-direction: the coodinate origin is chosen to coincide with the total c.m. Only one

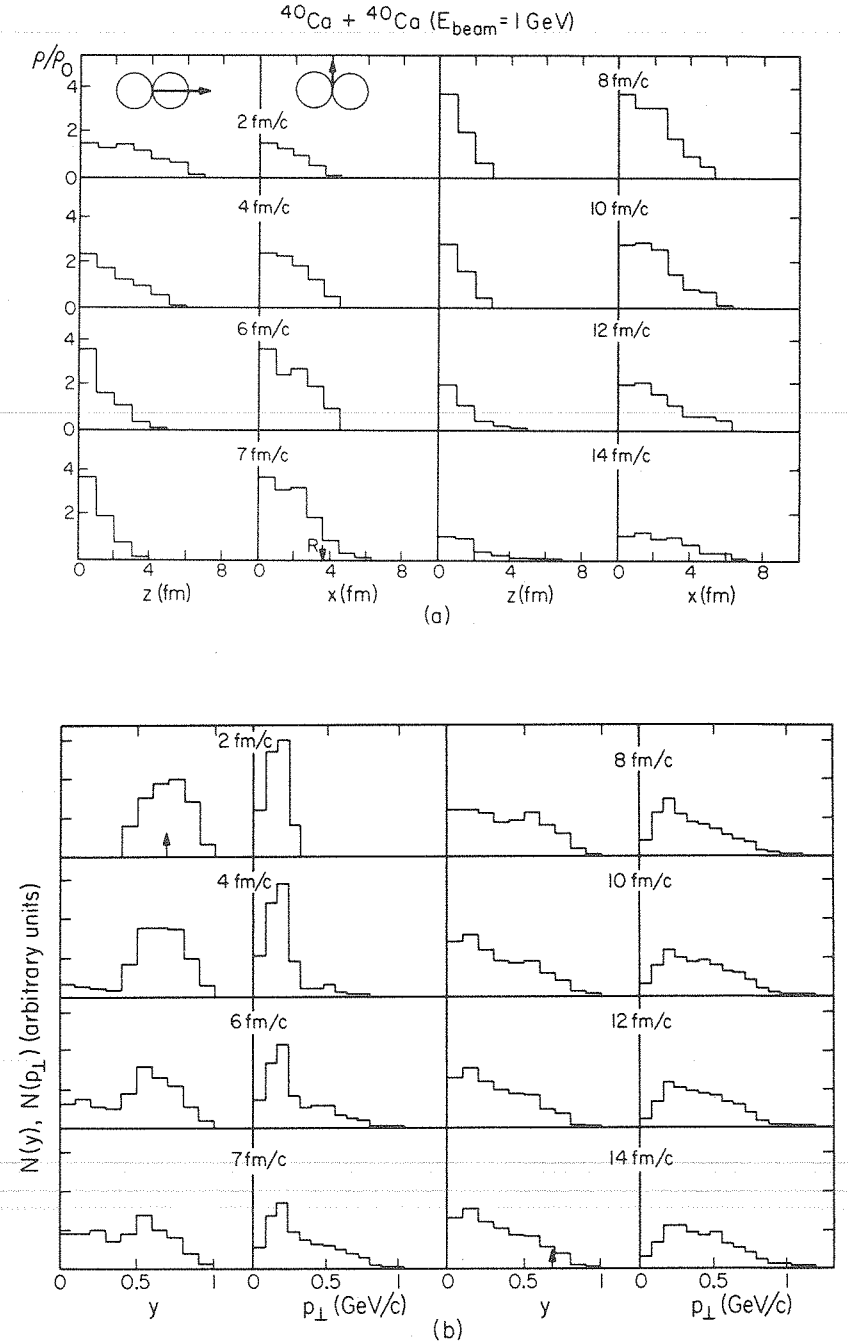

Fig. 3. $^{40}Ca + ^{40}Ca$, $b = 0$, $E_{beam} = 1$ GeV: (a) time evolution of the density profile along the lines shown at the top of the figure (see text also), R is the radius of ^{40}Ca, (b) time evolution of the rapidity and $p_\perp$ distributions. The arrow indicates the initial rapidity of the nuclei in the c.m. frame.

half of each profile is shown, as they are symmetric through the origin. We see that (i) along the beam direction nuclear matter is progressively compressed and reaches a maximum compression at roughly $t \sim 8$ fm/c (1 fm/$c \approx 0.33 \times 10^{-23}$ s). It is then decompressed rather quickly and becomes explosive towards the last stage of collision; (ii) from the z- and x-direction profiles one may observe that at the maximum compression ($6 \sim 9$ fm/c) the whole system looks like a pancake with radius almost equal to that of ^{40}Ca and a thickness of $4 \sim 6$ fm. (iii) There is no indication of appreciable side-splash up to $t \sim 8$ fm/c. Afterwards the matter seems to escape at roughly the same rates in both x- and z-directions. We will come back to this point later.

Fig. 4a shows the same type of profiles but for the case of $E_{\text{beam}} = 2$ GeV collision. As expected, the compression is higher and the explosive nature at the last stage is even more prominent. For both 1 and 2 GeV we find quick decompression but no appreciable side-splashing.

The present result confirms our previous work [3]): by looking at the density variation around the c.m., we have observed that the compression stage lasts approximately for 3 fm/c and that the decompression is very fast. Although it is not clear in figs. 3 and 4, there is a diving phase, during which the two nuclei interpenetrate each other almost freely (up to $5 \sim 6$ fm/c at 1 GeV) before the compression sets in. In order to get some idea about the duration of the various phases, similar calculations have been performed at 0.4, 0.6, 1.5, 2.5 and 3 GeV, respectively. As expected intuitively, all the phases (diving, compression and decompression) are shortened as the collision energy increases. For example, the diving phase almost disappears at 3 GeV.

The maximum density reached (in the total c.m. frame) is plotted in fig. 5. For model (CR) the compressibility (ρ/ρ_0) significantly exceeds the transparency limit 2γ (i.e., the density obtained by simply superposing the two Lorentz-contracted nuclei), where γ is the usual Lorentz factor for the nuclei in the cm. frame.

As we shall see in the next subsection, the two colliding nuclei eventually form after some time span (~ 8 fm/c) a system of nucleons, the dominant part of which is nearly at rest. This system is quite "hot": the nucleons have large random velocities, but on the average the system is at rest. Therefore, the baryon number density ρ obtained here does actually represent a property of a (combined) single nuclear matter (see, however, remark in sect. 4).

Our present result may be compared with that of a more simplified Monte Carlo calculation of Bondorf *et al.* [26]). Detailed features are certainly different because input quantities and kinematics are not the same. Yet, the similarity in the two models with regard to the time evolution in the baryon number density should be noted. Our results show a higher maximum density than that of model RIHC of ref. [26]) (the closest to our picture). This difference could be due to our inclusion of Δ-production (see our discussion below).

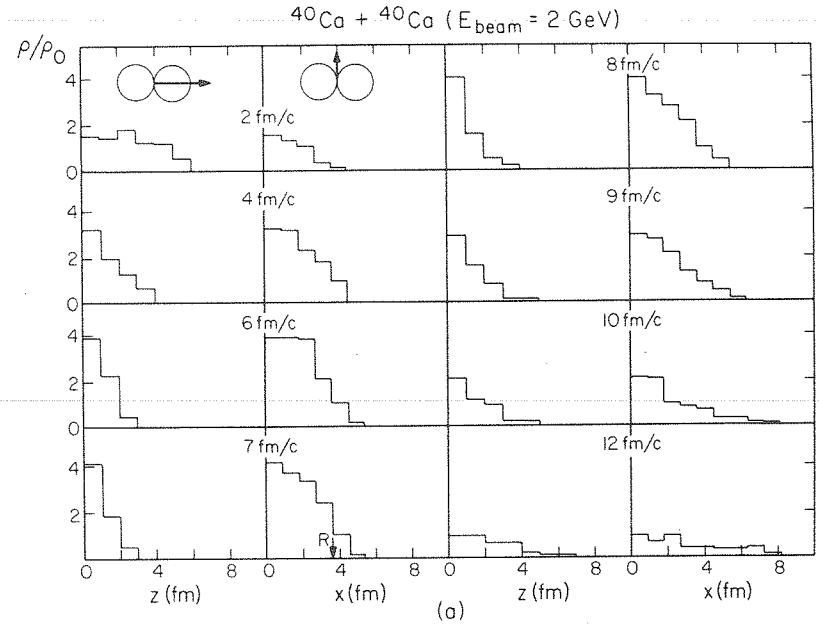

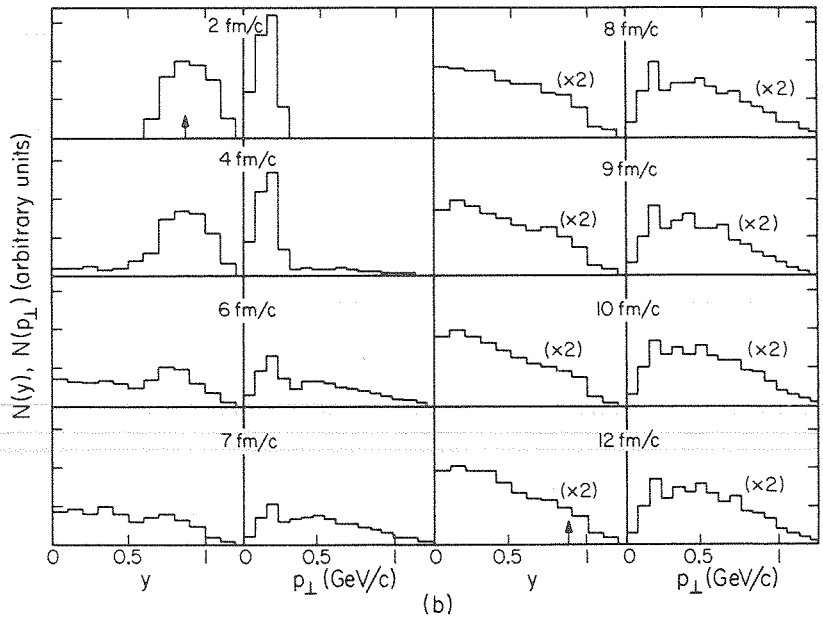

Fig. 4. Same as fig. 3 at $E_{\text{beam}} = 2$ GeV.

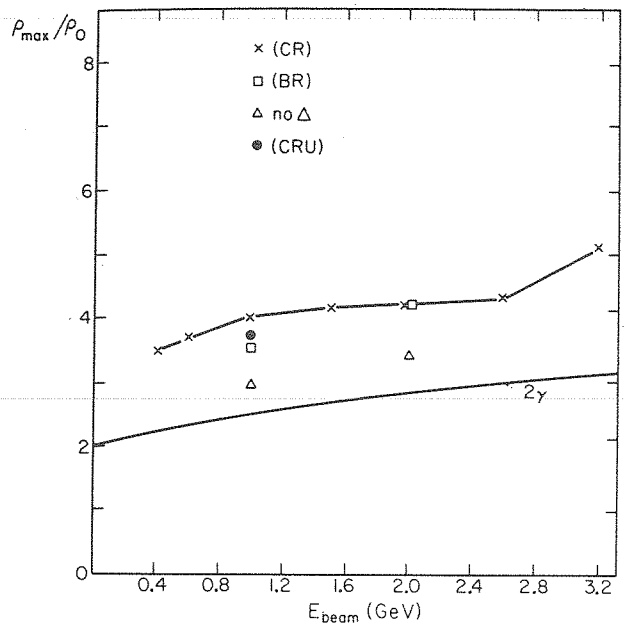

Fig. 5. Maximum density attained by the system ($^{40}Ca + ^{40}Ca$, $b = 0$), in the c.m. frame, as a function of E_{beam}. The symbols at the top of the figure correspond to several models for the Δ-behaviour (see text). The full line gives the density obtained by superposing the two nuclear densities.

3.2. MOMENTUM DISTRIBUTIONS

In figs. 3b and 4b we show the time evolution of the rapidity (y) distributions along the beam axis (the figures give one half of the spectrum only since it is symmetric) and of the transverse momentum ($p_\perp$) distributions for the baryons. Here, the model (CR) is considered for $E_{beam} = 1$ and 2 GeV, respectively. As is easily observed, the region of small rapidity is quickly populated in proportion to the rapid depopulation of the peak of the initial distribution and reflects the overall longitudinal slowing down of the nucleons. At the end of the compression stage ($t \approx 8 \sim 9$ fm/c) the initial peak has been fairly reduced. Thus, the compressed stage of the system can be viewed as a collection of baryons (roughly three-fourths of the system), excited but at rest, crossed by the remnants of the two initial opposite flows. As a consequence, the densities in fig. 5, reduced by one-eighth (see sect. 4 and fig. 15) approximately, are really an intrinsic property of the matter formed and do not result merely by superposing two nuclei running against each other.

Although the final spectra look very different from the initial ones [see figs. 3b and 4b], they are not fully thermalized: one may observe this in (i) the somewhat underpopulated spectrum for very small rapidity and (ii) the remnants of the initial maxima in both the y and $p_\perp$ spectra. Still one may clearly observe that the

longitudinal slowing down of the matter is rather efficient. The smaller the energy the more efficient it is, as one could intuitively guess.

We may compare the above result with the one of Randrup [18]), who studied the collision of two distinct infinite pieces of nuclear matter on the basis of the relativistic Uehling–Uhlenbeck equation. The matter equilibrates in a time shorter than 8 fm/c. The reason for a quicker relaxation in ref. [18]) compared with ours comes essentially from the spatial geometry: two incoming nuclei configurations reduces the frequency of the binary collisions.

Despite the fact that neither the y nor $p_\perp$ distributions show the fully thermal equilibration of the colliding system, we have tried to fit them with some appropriate thermal form in order to extract "effective" rapidity (or longitudinal) and transverse temperatures. This is done for various projectile energies as shown in fig. 6. The fits are made by relativistic Boltzmann distributions which are good approximations to Fermi-Dirac functions at the temperatures expected. For each projectile energy, we have also calculated the temperature, T_{gas}, the system would have acquired if it had thermalized as a classical, non-relativistic gas. ($T_{\text{gas}} = \frac{2}{3}K$, K being the available

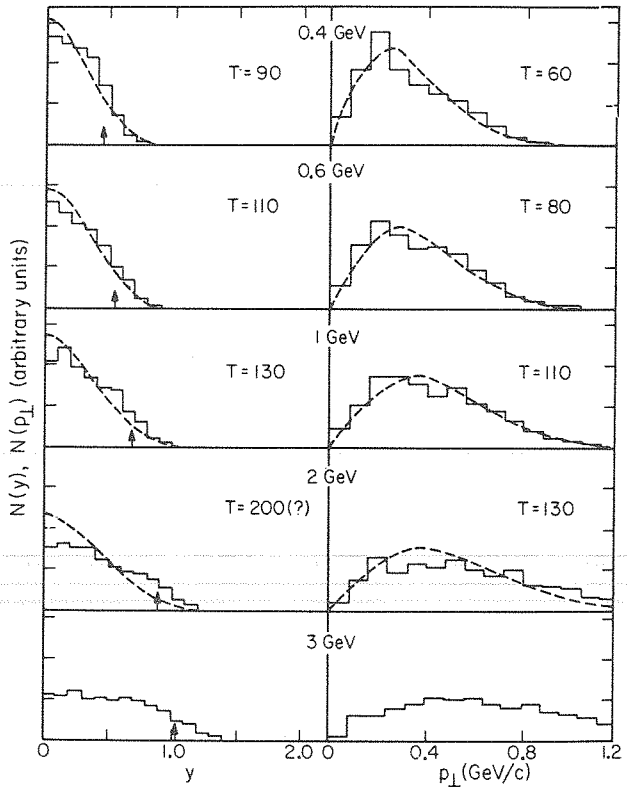

Fig. 6. ^{40}Ca+^{40}Ca, $b = 0$. Final nucleon y and $p_\perp$ distribution at various beam energies. Dotted lines are fits to Boltzmann distributions with the indicated temperatures.

kinetic energy per nucleon). The sensitivity of the fits is such that the transverse temperatures T_y are determined within an accuracy of 10 MeV, while typical uncertainties in the longitudinal temperatures ($T_\perp$) are between 20 and 30 MeV.

It appears from our results that (i) generally $T_y > T_\perp$ showing that the system does not attain equilibrium (ii) both T_y and $T_\perp$ are lower than T_{gas}, notably for high incident energy, which demonstrates the fact that Δ-production efficiently removes translational energy from the nucleonic system and consequently cools it down (see fig. 9).

Incidently, we should mention that for $E_{beam} > 1.5$ GeV the longitudinal temperature exceeds the so-called Hagedorn temperature [22]) $T_H \approx 140$ MeV, i.e., the pion mass. One might argue this as indicating the limitation of our model. However, noting the uncertainty in T_y mentioned above and furthermore remembering that the extracted temperatures have only tentative meaning, the model is probably applicable up to $E_{beam} \approx 2$ GeV. At higher energies, more baryon resonances must be included in addition to multi-pion production in single NN scattering.

The relatively weak coupling between longitudinal and transverse motion is depicted in a more dramatic manner by fig. 7 (upper part), where the final value of the asymmetry parameter Y is given for different incident energies:

$$Y = \frac{\langle p_\perp^2 \rangle}{\langle p_\parallel^2 \rangle}, \tag{3.1}$$

where the bracket stands for the average over momentum distribution. For a complete thermal equilibrium, Y is equal to 2. Our Y's are considerably lower, even for collisions at relatively low energy, which shows that the system is not fully equilibrated. The lower part of fig. 7 gives a typical time evolution of Y. At the beginning Y has a value near, but not equal to, zero because of the Fermi motion. It remains small for some time, presumably because half of the first collisions are high-energy elastic (and thus very forward-peaked) collisions. When secondary collisions become dominant, momentum is transferred in the transverse direction and makes Y grow rapidly. This quantity keeps growing until the fast decompression of the system abruptly decreases the "luminosity", i.e., the number of binary collisions per unit time. This is clearly seen in the lower part of fig. 7, although there seems to be some shift between the times at which dY/dt and the luminosity vanish. This is probably due to the fact that the collisions are fairly soft at the end of the interaction process. From fig. 7, one could guess that, if the system did not decompress, Y would change from its initial value to a value around 2 in a time span ≈ 10–12 fm/c, which agrees fairly well with the result of Randrup [8]). It is interesting to note that the interaction process stops at a time (~ 10 fm/c) when the average density of the system returns to nuclear matter density at equilibrium. We want to stress that in actual systems, the strong interaction (in the sense of the interaction felt by baryons) is not likely to switch off completely after this time. Most

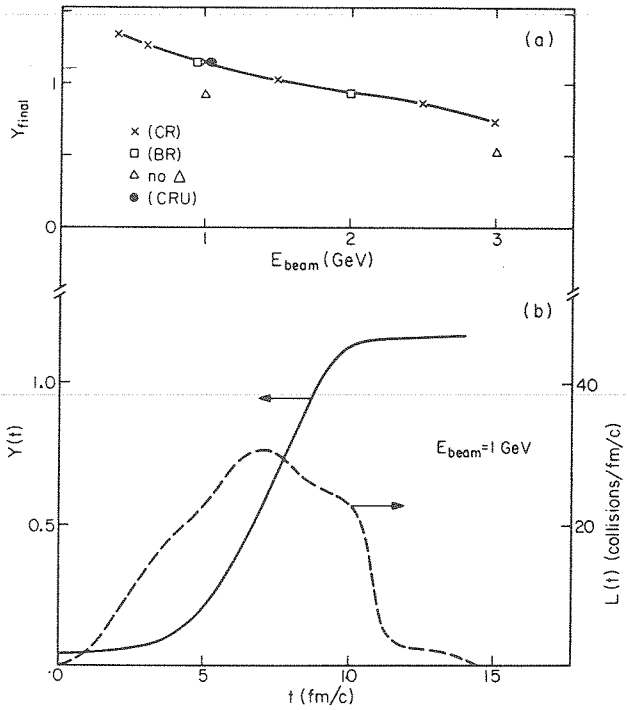

Fig. 7. $^{40}Ca+^{40}Ca$, $b=0$. (a) Final asymmetry of the nucleon momentum distribution as a function of the beam energy. (b) The full curve is the asymmetry parameter Y as a function of time for $E_{beam}=1$ GeV. The dotted curve represents the luminosity.

probably it goes on to manifest itself, not in a pattern of binary collisions as we describe it here, but in an average nuclear field which will tie nucleons in clusters. This is, of course, beyond the scope of our model.

3.3. PION MULTIPLICITIES AND PION SPECTRA

As mentioned before, we have assumed that the pions are produced via Δ-particles and that the latter decay at the end of the collision process. The decay is assumed to be isotropic in the Δ-rest system. In fig. 8 the average multiplicity is given as a function of the initial collision energy. The curve deviates from zero somewhat below the Δ-production threshold for the NN system (~600 MeV) due to Fermi motion inside the nuclei. After an almost linear increase, the curve is less steep around $E_{beam}=2$ GeV and flattens around 3 GeV.

As noted in refs. [28,29]), the Δ-recombination ($N\Delta \rightarrow NN$) seems important at low energy. The reason is that the lower the incident energy is, the lower the energy of the Δ is and the higher the recombination cross section is. We checked [see also ref. [3])] that Δ-recombination reduces the multiplicity by 30% at $E_{beam}=1$ GeV. At energies

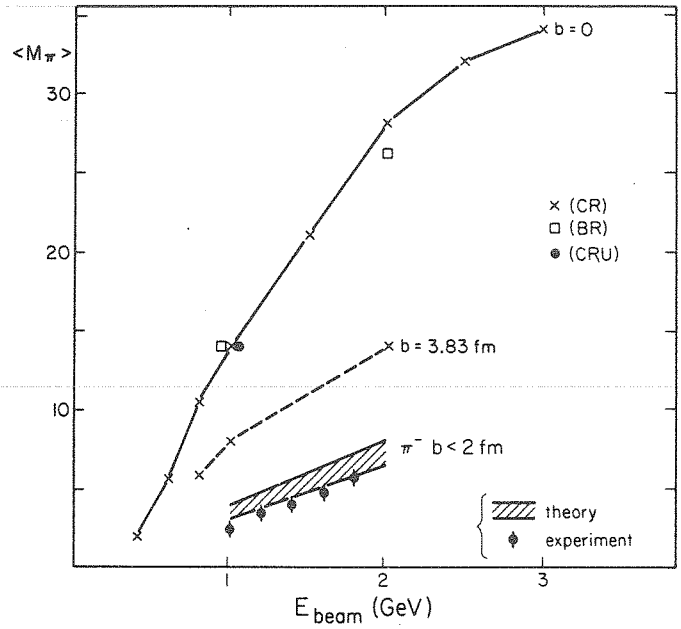

Fig. 8. Average pion multiplicity as a function of the energy. The sashed area represents the prediction of the model for the π^- multiplicities in collisions with impact parameter $b \leq 2$ fm (see text). The experimental data are from ref. [25]).

lower than 500 MeV this effect is likely to be in excess of 50%, while above 2 GeV it is probably rather small and fairly constant.

Since we have assumed a complete isospin degeneracy of the system and Δ-resonance dominance, the multiplicity of a certain type of pion, say π^-, should be understood as *one third* of the pion multiplicity that we have obtained. We compare our result with the streamer chamber measurement for the Ar+KCl system [30]). At $E_{beam} = 1.8$ GeV for instance, our estimate $n_{\pi^-} \approx 7$ is somewhat higher than the experimental one $n_{\pi^-}^{exp} \approx 5.7$ (for an average over impact parameters ≤ 2 fm, according to the authors). This overestimate was expected from the isobar picture we adopted. We assumed that the Δ-production cross section is the same for any pairs of nucleons (nn, pp, np) and is equal to the experimental inelastic cross section. However, the np pair is half a $T = 1$ state and half a $T = 0$ state. The latter is not able to decay in a NΔ configuration because of isospin conservation. Hence, we overestimate the Δ-production coming from the np pairs. The effect is likely to be of 10–20% and will bring the results of the calculation closer to the experimental data (from the upper limit to the lower limit of the shaded area in fig. 8). We recall that model A [see sect. 2 and ref. [3])] yields too large pion multiplicities by about a factor 2.

In the same way as for the protons, we have fitted the y and $p_\perp$ pion spectra with Boltzmann thermal distributions. Once again the spectra (not shown) are not exactly thermal. Moreover, they have less statistics than the proton spectra, for obvious

reasons, and the temperatures are determined with less accuracy. Nevertheless they are quoted in fig. 9 along with the proton temperatures. It turns out that the y-temperatures seem higher than the transverse temperatures, except at low energy, and both are lower than the corresponding ones for baryons. In ref. [31]), such a feature has tentatively been ascribed as an indication of a blast wave. However, this feature can alternatively result from the decoupling between a Δ-particle gas and a nucleon gas which have been in thermal equilibrium for a while. The Δ's then decay and the produced pions get a "temperature" smaller than the one of the nucleons.

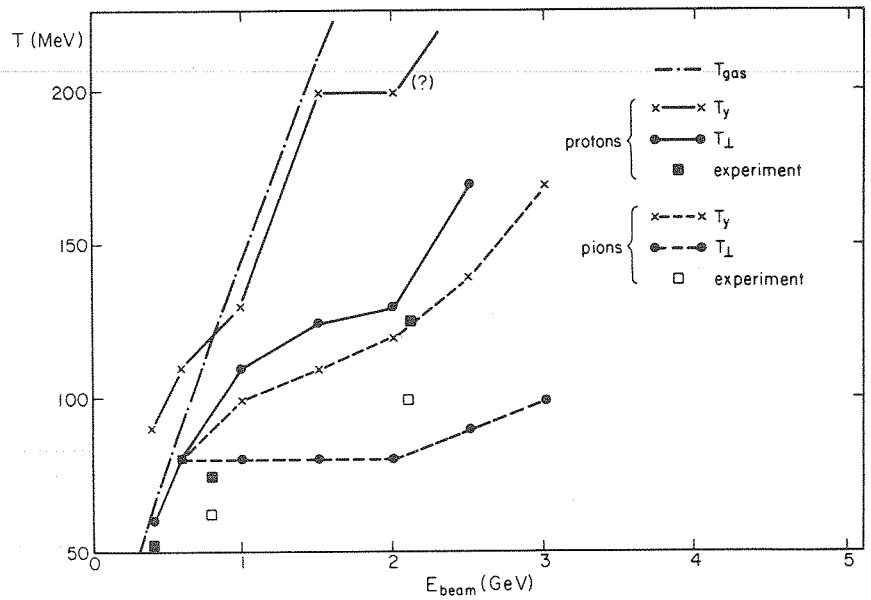

Fig. 9. Proton and pion longitudinal and transverse temperatures. The squares are the experimental data of ref. [27]). The dot-dashed curve is the equilibrium temperature for an ideal non-relativistic gas.

We have shown in fig. 9 the "temperatures" extracted from the 90° c.m. inclusive cross sections [32]). The system involved is Ne+NaF, but they are not expected to differ very much for the system we study. They should be compared with our transverse temperatures. The agreement is satisfactory in view of the uncertainty on our values and the fact that experimental temperatures are taken from the high-energy tail of the inclusive cross section only whereas our are determined by the whole spectrum.

Although this may not be transparent from fig. 9, the asymmetry parameter Y of the pion momentum distribution is considerably larger than the corresponding final quantity for the proton (fig. 7). It stays close to 2 up to $E_{beam} = 1$ GeV and then decreases a little bit.

3.4. ROLE OF THE Δ-PARTICLES

Before discussing the role of the Δ's, it is interesting to look at the time evolution of the number of Δ-particles, as shown in fig. 10. It has the same shape for all energies: an almost linear increase to a maximum, no change for a short period and then a small decrease towards the final value. This behaviour can be interpreted qualitatively as follows. The rate of Δ-production is roughly given by

$$\frac{\mathrm{d}N_\Delta}{\mathrm{d}t} \approx N\rho\sigma_1(\bar{v}_1)\bar{v}_1 - N_\Delta\rho\sigma_2(\bar{v}_2)\bar{v}_2$$

$$\approx \rho[N\sigma_1(\bar{v}_1)\bar{v}_1 - N_\Delta\sigma_2(\bar{v}_2)\bar{v}_2], \tag{3.2}$$

where N is the number of nucleons in the interaction volume (which involves a large fraction of the system after a while), $\sigma_1(\sigma_2)$ is the production (recombination) cross section and $\bar{v}_1(\bar{v}_2)$ is the average relative nucleon–nucleon (nucleon-Δ) velocity. At the beginning the first term overtakes the second one. For some time, say the diving stage (up to $\sim 6.7\,\mathrm{fm}/c$ at $1\,\mathrm{GeV}/A$), it stays roughly constant, since most NN collisions have essentially the same kinematics as the one of the nuclei: $\bar{v}_1$ is then close to the nucleus–nucleus relative velocity. But, in the compression stage, the thermalization sets in and the average velocity is diminished accordingly. As a consequence, $\sigma_1(\bar{v}_1)$ is reduced dramatically. On the other hand, the second term in eq. (3.2) is growing up because N_Δ has increased and because $\bar{v}_2$ goes down bringing $\sigma_2(\bar{v}_2)\bar{v}_2$ to higher values (see fig. 1). One may guess from figs. 10 and 3 [see also ref. [3])] that the second term in eq. (3.2) is the dominant one at the end of the compression stage and is driving the number of deltas down to what would be its equilibrium value if the density and temperature prevailing around $8\,\mathrm{fm}/c$ did not change any further. This value is possibly not reached, because the decomposition stage is very fast and the density quickly vanishes. We can guess approximately this equilibrium number of Δ's from fig. 9. We would have roughly

$$\left(\frac{N_\Delta}{N_\mathrm{p}}\right)_{\mathrm{eq}} \approx 4\exp\left[-\frac{m_\Delta - m_\mathrm{p}}{T}\right]. \tag{3.3}$$

For example, at $E_{\mathrm{beam}} = 1$ GeV, we can take $T \approx 100$ MeV, a value intermediate between the longitudinal and the transverse temperatures. Hence $(N_\Delta)_{\mathrm{eq}} \approx 12$, while N_Δ becomes equal to 14 at the end of the interaction process. We can conclude from these considerations that the pion multiplicities have possibly recorded some properties of a quasi-equilibrium state of the system before its decompression.

We now want to discuss the role of the Δ's in the interaction process. First we examine how the compression of the matter is influenced by the Δ-production. For this purpose we have repeated the calculation by switching off the Δ-production: the NN scattering is elastic at all energies with the actual total cross section. The results for $E_{\mathrm{beam}} = 1$ and 2 GeV are shown in fig. 5 by small triangles. We clearly observe

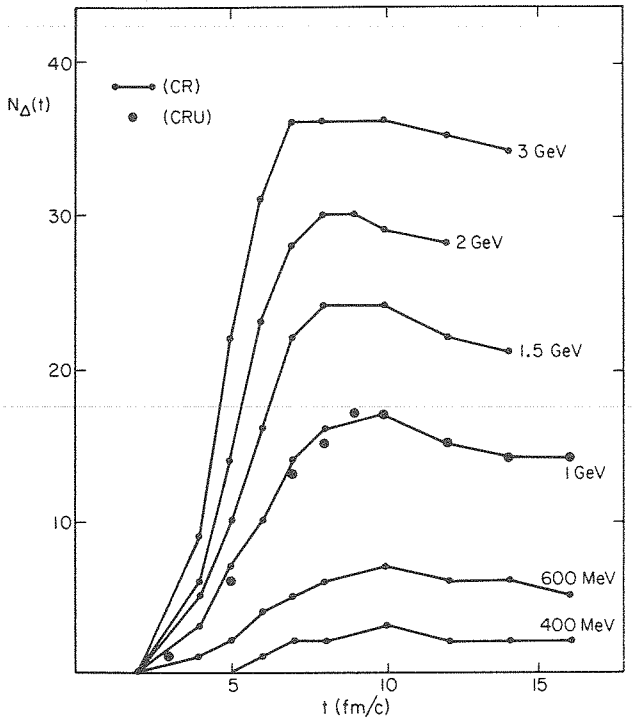

Fig. 10. $^{40}Ca + ^{40}Ca$, $b = 0$. Time evolution of the number of Δ-particles.

that the introduction of Δ-particles makes the compression higher. Such a possibility was predicted a long time ago on the basis of simple arguments [33]). In terms of hydrodynamics, the reason for the Δ's playing this role may be clear: the introduction of an endothermic process into the system generally makes the equation of state softer, thus higher compression can be attained. Specifically, the creation of Δ-particles slows down the original fast longitudinal motion quite efficiently so that the piling up of the two slabs of nuclear matter (initially moving fast against each other) gets easier, resulting in higher compression.

The role of the Δ-particles in thermalizing nuclear matter seems even more crucial. We may understand this by comparing the final y and $p_\perp$ distribution of nucleons as calculated from the model with and without Δ's (figs. 6 and 11, respectively). We find that Δ-production makes the y-distribution closer to thermal equlibrium, especially at 2 GeV. On the other hand, the $p_\perp$ distributions are not very much influenced by the Δ-inclusion. The reason is that Δ-production does not bring more transverse momentum than NN elastic scattering does. In fact, on the average, it brings less. Consider, for instance, the initial, most important, collisions, neglecting for a while the Fermi motion. At $E_{\text{beam}} = 1$ GeV the incoming nucleons have a (longitudinal) momentum of 0.69 GeV/c in the c.m. system. If they are scattered elastically at

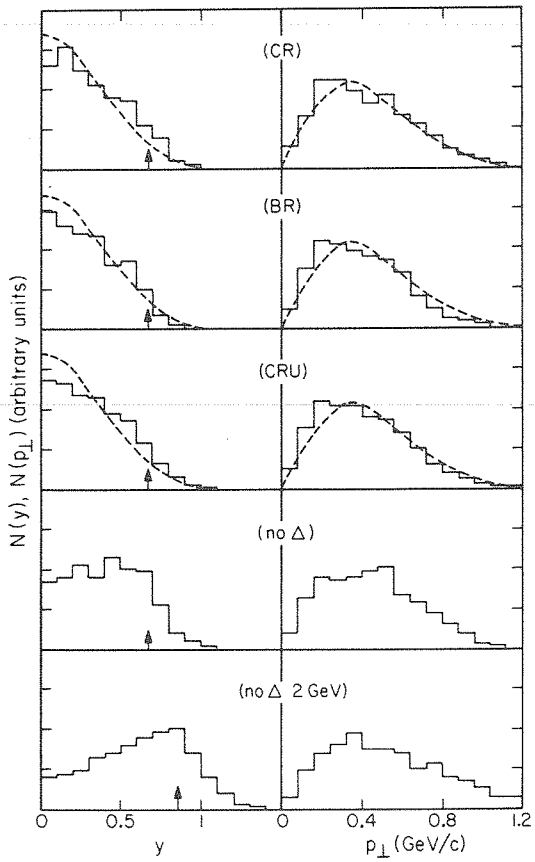

Fig. 11. $^{40}Ca+^{40}Ca$, $b=0$, $E_{beam}=1$ GeV. Final nucleon y and $p_\perp$ distributions for various models of Δ-behaviour (see text).

$\theta_{cm}=90°$, they can acquire a transverse momentum of that amount. However, this happens very rarely and if we refer to the actual angular distribution [eq. (2.2)], we can say that, in the average, they are scattered with a transverse momentum of the order of 0.30 GeV/c. If a Δ-particle is produced through the collision, the two outgoing particles will have a momentum of 0.34 GeV/c. As they are produced isotropically in our model, their average transverse momentum will be around 0.25 GeV/c. Hence, the isotropic angular distribution of the Δ-production alone *does not help* the system to randomize. This statement is supported by the results of a calculation in which we used an angular distribution for the Δ-production (and recombination) cross section of the form given by eq. (2.2), $A(s)$ being kept the same. There is some experimental suport [34]) for such a choice. Note that, in this case, t is not minus the squared 3-momentum tranfer any longer. Rather, it is given by

$$t=2m^2-2[(q_i^2+m^2)(q_f^2+m^2)]^{1/2}+2q_iq_f\cos\theta\,, \tag{3.4}$$

where q_i, q_f are the initial and final c.m. momentum respectively, m is the nucleon mass and θ is the scattering angle in the c.m. At the threshold, $q_f \to 0$, and the Δ-production becomes isotropic. The calculated final y and $p_\perp$ distributions at $E_{beam} = 1$ GeV, using such a choice [this model is referred to as (CRU) in the figures], are shown in fig. 11. They are identical to the results with model CR within the uncertainties of the calculation. This is equally true for the evolution of the y and $p_\perp$ distribution (not shown), for the pion multiplicity (fig. 8), for the final asymmetry coefficient Y (fig. 7), for the evolution of the number of Δ-particles (fig. 10) and for the pion temperatures (not shown). There is, however, a small difference as far as the maximum density is concerned (fig. 5).

All these arguments lead to the conclusion that Δ-production mainly acts to slow down quite efficiently the two incoming fluxes of nucleons along the mean trajectories by transforming longitudinal kinetic energy into mass energy.

Eventually, the Δ's may also help in randomizing through the elastic scattering by the nucleons and through the recombination (and subsequent creation) process. We have checked that elastic scattering is not important in that respect, as shown in fig. 11, where several results from calculations with model BR are plotted. We recall that in this model, elastic scattering of the Δ's is neglected, whereas recombination is taken into account. They are very similar to those obtained with model CR. The same situation also holds for the compression (fig. 5), the asymmetry of the nucleon momentum distribution (fig. 7) and the pion multiplicity (fig. 8). This is a fortunate feature of the model, since the N-Δ elastic scattering cross section is not known experimentally.

Finally, we can summarize our discussion by saying that the transfer of the initial available energy into the perpendicular motion is not very efficient (see the difference between $T_\perp$ and T_{gas} in fig. 9). The Δ-particles do not play any significant role in that transfer. They, however, do play a crucial role in thermalizing the system along the longitudinal direction. They do that mainly in transforming longitudinal kinetic energy into mass energy, cooling the system in such a way. Fig. 9 substantiates this statement. If the nucleons equilibrized in the longitudinal direction without inelasticity and had transverse temperature shown in the figure, their longitudinal temperature would be $T_y \approx T_{gas} + 2(T_{gas} - T_\perp)$ (in the non-relativistic approximation), i.e., much higher than T_{gas}. The Δ-production pushes T_y down below T_{gas}. More quantitatively, the inelasticity can be characterized by the ratio of the total energy contained in the pion system at the end of the process (W_π) to the available kinetic energy in the c.m. system (K_a). These values are contained in table 1. The inelasticity increases with energy, as expected, but tends to stabilize around 2 GeV.

4. Non-central collisions of two $A = 40$ nuclei

We now turn to the collision of two ^{40}Ca-like nuclei with a non-zero impact parameter. Specifically we shall first study the case where $b = 3.83$ fm, a value equal

TABLE 1

Inelasticity for the $^{40}Ca+^{40}Ca$ system, $b=0$

E_{beam} (GeV)		0.6	1.0	2.0
$\frac{W_\pi}{K_a}$	CR	0.14	0.23	0.28
	CRU		0.27	

to the radius of each nucleus. In fig. 12, we show some snapshots of the density distribution given at $t=8$, 11 and 14 fm/c for the case of $E_{beam}=1$ GeV. The curves are equidensity contours of the baryon number density in the reaction plane. The size of the mesh is twice as small as before and the distribution has been symmetrized by averaging over the calculated one and its image inverted through the c.m. Curves are obtained by interpolation from the values at the mesh points. The density is

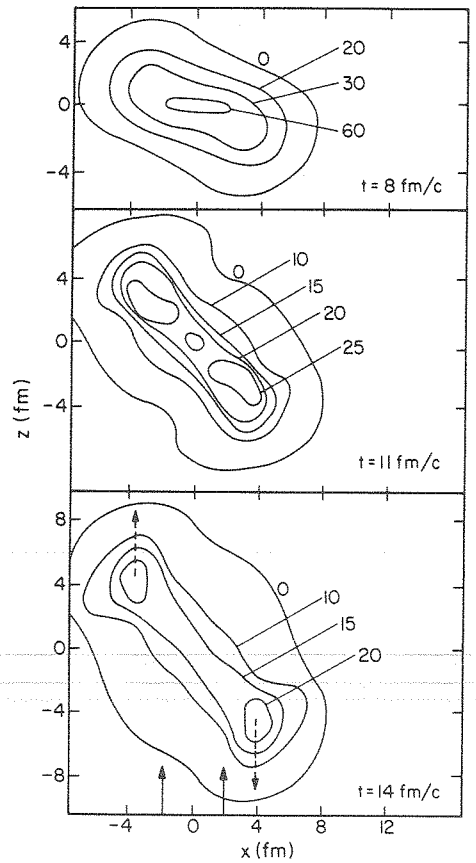

Fig. 12. $^{40}Ca+^{40}Ca$, $b=3.83$ fm, $E_{beam}=1$ GeV. Contour plot of the density in the reaction plane. The arrows at the bottom of the figure give the geometrical cut between spectator and participant matter. The dotted arrows indicate the general motion of the spectator parts. The density is given in $\frac{1}{18}\rho_0$ units.

measured in units of $\frac{1}{18}\rho_0$ ($\rho_0 = 0.17$ fm^{-3}; the normal nuclear matter density). One can see that the system still achieves a high density in the c.m. region at a time around 8 fm/c. The maximum density is smaller than the corresponding one in a central collision (see fig. 5), as one could have guessed, since less matter can be piled up, but it is still higher than the transparency limit.

Fig. 12 strikingly supports the participants-spectators picture of high-energy collisions. We have indicated at the bottom of the figure the cut implied by the simplest fireball model. One clearly sees two pieces of matter with (asymptotically) the normal nuclear matter density travelling with almost the initial velocity. The central part of the system is very excited. There is not, however, a very clean cut between the participants and the spectators, mainly because the central part is expanding. Up to 14 fm/c this leads to a kind of "dog's bone" shape.

We investigate the validity of the participants-spectators picture a little bit further by looking at the matter density for later times. This is shown in fig. 13. Here, what is

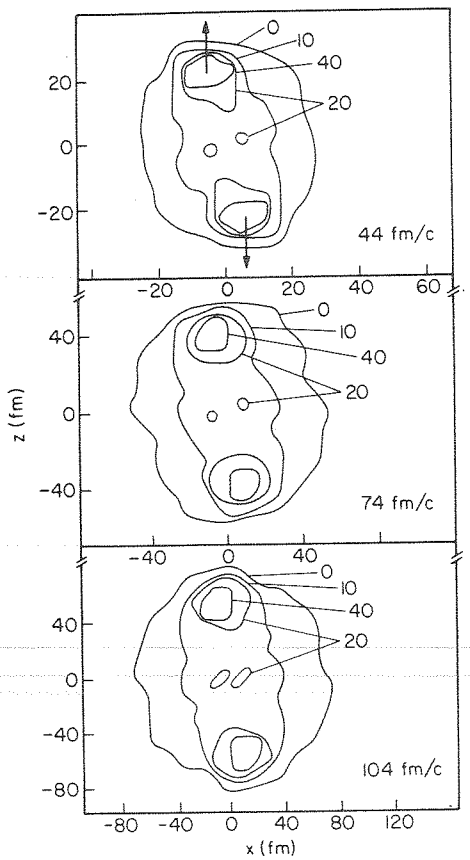

Fig. 13. ^{40}Ca+^{40}Ca, $b = 3.15$ fm, $E_{\text{beam}} = 1$ GeV. Contour plot of the density integrated along the direction perpendicular to the reaction plane for later times. Note the change of scale. The density unit is 2.26×10^{-3}, 7.7×10^{-4} and 3.85×10^{-4} fm^{-2}, respectively, from top to bottom.

plotted is the baryon density integrated along the direction perpendicular to the reaction plane. The center keeps expanding, becoming dilute at $t \approx 100$ fm/c. The spectator parts also expand, but at a smaller rate. The latter is a straightforward consequence of our neglect of an average field. In nature, the average field will keep the nucleons closer to each other. However, the spectators are frequently fragmented. Hence, we do expect that the extension of the spectator parts in our picture will be close to the physical reality, although the details of the matter density for these parts are probably wrong.

The successive patterns of the matter density can be fitted rather nicely by a sum of a central gaussian and of two Lorentz-contracted gaussians,

$$\rho(r) = \frac{A_p}{(r_0\sqrt{\pi})^3}\exp\left(-\frac{r^2}{r_0^2}\right) + \frac{1}{2}\frac{(A-A_p)\gamma}{\pi^{3/2}a^3}\left[\exp\left(-\frac{(x-x_1)^2+y^2+\gamma^2(z-z_1)^2}{a^2}\right)\right.$$
$$\left.+\exp\left(-\frac{(x+x_1)^2+y^2+\gamma^2(z+z_1)^2}{a^2}\right)\right], \qquad (4.1)$$

where γ is the Lorentz factor associated with the nuclei in the c.m. frame, and A is the total nucleon number of the system. We have adjusted the parameters A_p, r_0, x_1, z_1 and a to reproduce several of the first moments of the distribution. This operation is repeated for several times. Typical results of the fits are given in fig. 14 for a slightly different impact parameter ($b = 3.15$ fm). One can see that A_p is fairly constant, except for the earliest times, when the separation between spectators and participants is not yet clear. The quantities z_1, a, r_0 are linear functions of time. In

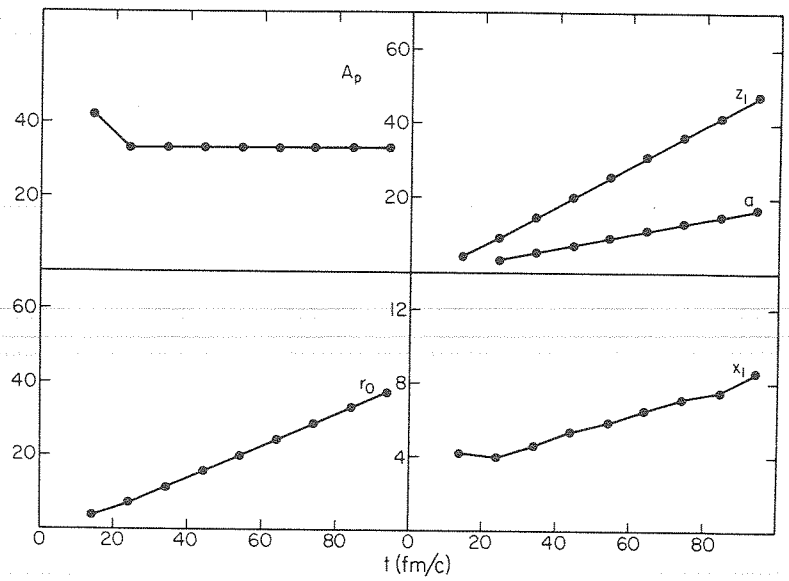

Fig. 14. Parameters of the fit to the density as functions of time (see text).

particular, the rate of increase of z_1, which is the velocity of the spectator parts, is close to but slightly smaller than the velocity of the incoming nuclei. The quantity x_1 increases slowly, indicating that the participants are kicked sidewise. In a clear-cut model, x_1 would be always very close to the radius of the nuclei, i.e., 3.83 fm. Hence, fig. 14 indicates a small sidesplash in a direction around 5° off the beam direction. The angle is probably too small to leave a neat mark in the inclusive cross sections [4]). The situation would be more favourable for an asymmetric system like $^{20}Ne+^{235}U$, where maxima around 30° have tentatively been interpreted as sidesplash evidence [14]).

Whereas our model qualitatively agrees with the spectator-participant picture, there is a systematic discrepancy, as shown in fig. 15, where the value A_p is plotted as a function of b. It is always smaller than the prediction of a clear-cut geometry picture, as the one used in the fireball and the firestreak models. The difference is particularly evident in central collisions, for which our model predicts a substantial amount of transparency (this is, however, expected to decrease for heavier systems).

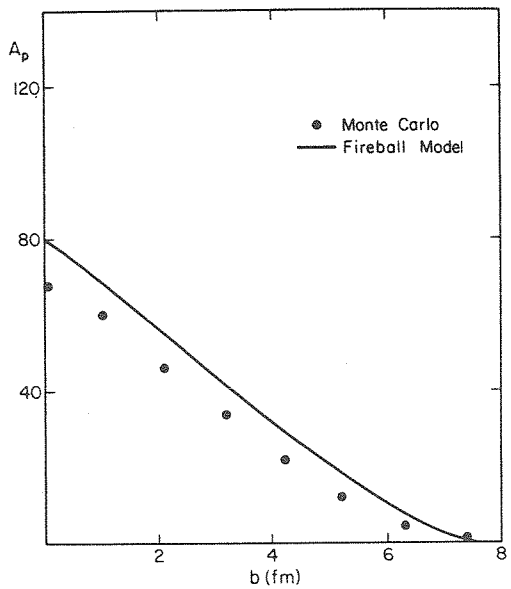

Fig. 15. Number of participants as a function of b.

Fig. 16 displays the final y and $p_\perp$ distributions for a 3.83 fm impact parameter. The dashed curves correspond to thermal spectra with the same temperatures as the ones we extracted for the central collisions and with a normalization corresponding to the value of A_p of fig. 15 ($\approx$30 for $b = 3.83$ fm). As is especially clear from the $p_\perp$ distribution (less from the y-spectrum), the system is divided into a hot piece of A_p nucleons (with a temperature apparently indepenent of b) and of a part which is

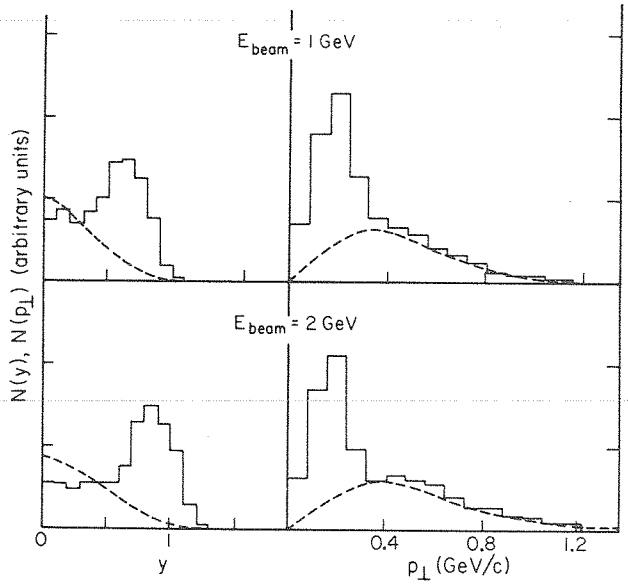

Fig. 16. $^{40}Ca+^{40}Ca$, $b = 3.83$ fm. Final nucleon y and $p_\perp$ distributions.

almost cold: its spectrum is almost identical to the orginal spectrum of the system (see figs. 3 and 4).

As for the pions produced, we find that (i) the multiplicities are decreasing functions of the impact parameter. For 1 GeV/A, they closely follow a gaussian law, $\exp(-b^2/b_0^2)$, with $b_0 = 4.7$ fm. Multiplicities for $b = 3.83$ fm are shown in fig. 8. (ii) The fit to the pion y and $p_\perp$ spectra yields essentially the same temperatures as those extracted in head-on collisions.

5. Central collisions of ^{20}Ne on ^{60}Ni

Our last case study is for central ($b = 0$) collisions but in an asymmetric system. What we have in mind specifically in this respect is to see if we can observe some features of possible shock waves. We have chosen ^{20}Ne and ^{60}Ni as the projectile and the target, respectively. The calculation has been carried on in the lab system. The result for $E_{\text{beam}} = 1$ GeV is shown in fig. 17 which averages over 40 runs. We plot the baryon number density along the beam (z) axis, with $z = 0$ as the center of the target.

Fig. 17 indicates that the projectile penetrates the target nearly freely up to 5 fm/c. Then a shock wave develops and propagates until about 10 fm/c. By shock wave, we mean that a strong discontinuity appears in the density profile, with a maximum higher than the mere superposition of the two original densities. The width of the disturbance is slightly smaller than the projectile diameter. In our case, the shock sweeps almost all the matter out, leaving behind it a small residue of matter only. It is also worthwhile to notice that the shock slightly disturbs the matter up to several fm

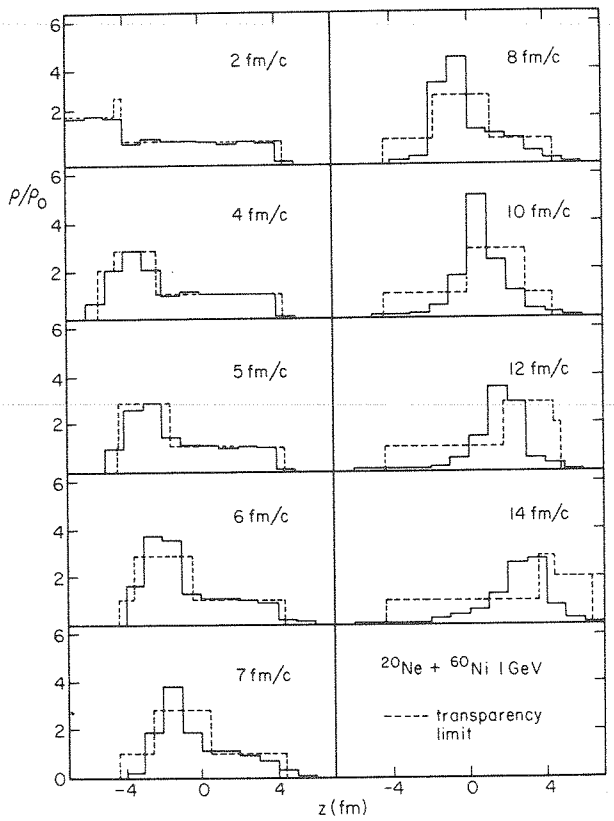

Fig. 17. ^{20}Ne + ^{60}Ni, $b = 0$, $E_{\text{beam}} = 1$ GeV/A. Density profile along the axis of symmetry in the target rest frame.

ahead of its forward front. After 10 fm/c, the compressed matter contained in the shock explodes and disperses all the nucleons.

The matter distribution off the z-axis reveals that, up to ~8 fm/c, the process can be seen as a projectile travelling almost undisturbed (except for the remarks made above) through the target. During that period, the majority of the target nucleons hit by the projectile are ejected sidewise. After $t \sim 12$ fm/c, all the nucleons in the system are dispersed preferentially in the forward direction. The combined result of these two processes is that the angular distribution of the final nucleons does not show any noticeable enhancement at $\theta_{\text{lab}} \neq 0$, contrary to the results of some hydrodynamic calculations [35]).

At 2 GeV (not shown), it turns out that the shock front almost passes through the target before disintegrating. During the travel, it is slowed down considerably: its rapidity goes down from 1.8 to ~0.8.

Finally, we mention that the total pion average multiplicity in this reaction has been found equal to ~10 at 1 GeV and ~19 at 2 GeV. Those values are lower than

the corresponding ones in the symmetric system of the same mass (^{40}Ca + ^{40}Ca). But, their ratio is constant and close to the ratio of the participant nucleons.

6. Discussion and conclusion

In our present study in relativistic heavy-ion scattering, we have been particularly interested in how the possible thermal equilibrium in colliding nuclear matter is approached. We have seen that the real equilibrium is never reached even in the most favourable case of a collision between two identical nuclei at zero impact parameter. We have also observed that introducing pion production through the Δ-production process helps the system to attain equilibrium, but not enough. The equilibration process is stopped by a rapid decompression of the system, which inhibits baryon–baryon collisions. Our model relies basically on the assumption that the two-baryon classical collisions regime is attained. Although this is largely believed to be true at the energies investigated here (or at least at energies higher than 1 GeV), there is no real justification available of this assumption. Other assumptions, less critical, can also be questioned. The model can possibly be improved by carefully studying the sensitivity of the results to these assumptions. We have already shown that choosing an isotropic Δ-production is not restrictive, since the results are largely independent of the precise shape of the Δ-production within reasonable variation of this shape. Removing the isospin degeneracy will probably improve the results for the pion multiplicities, as we explained in sect. 3. An important point is the behaviour of the Δ-particles. The description we adopted in this work is a compromise between a search for a simple model and the present knowledge of this problem. However, it would be highly desirable to check, even in a simple model, the accuracy of our picture.

We summarize our other findings in connection with various currently investigated problems.

(i) A collective sidesplash is confirmed by our calculation. It is, however, quite small for a symmetric system (^{40}Ca + ^{40}Ca). Preliminary results on ^{20}Ne + ^{60}Ni seems to indicate that the matter is diverted to larger angles for a non-symmetric system, although the angle is smaller than suggested by the calculation of Nix *et al.* [14]) and possibly by the experiment [35]). Yet, the two results may not really contradict each other as the latter deals with relatively low-energy cases ($E_{\text{beam}} = 250$ MeV). (ii) We have found, in our calculation, that for the case of head-on collision between ^{20}Ne and ^{60}Ni a strong shock wave develops. The possible existence of shock waves in nuclei is very controversial. Although it has been claimed on very general arguments [36]) that the shock front should be many times as thick as the mean free path of the nucleons, our results do not have this feature. We have no clear explanation for this at the moment. It might be the inelastic Δ-production process, which could make the analysis inapplicable. In our calculation, the shock wave disintegrates in a manner that does not produce any side-peaked distribution of the

final nucleons. (iii) There is presently some controversy about the possible existence of blast waves. We definitely observe in our calculation a very rapid decompression, although it does not take the form of a clear wave front travelling outwards. Moreover, the lower temperatures for the pions compared to the protons temperatures might not be an indication of a blast wave, as suggested in ref. [31]), but might rather come from the decay of Δ-particles which survive to the end of the strong interaction process. This possibility has already been pointed out in ref. [37]). (iv) Our Monte Carlo approach in its present construction does not allow for the incorporation of density isomerism [38]), multipion cluster mechanisms [39]) or pion field coherence [40]). (v) As in (iv) above, our present model is too simple to account for a detailed description of possible pionic instabilities. One may, of course, use a simplified picture: introducing some enhancement factor for the nucleon–nucleon cross section as a function of nuclear matter density [41]). Although this does not describe the interaction of nucleons with the strong pion field, it allows, to some extent, to search for a possible influence of the instabilities on the nucleon momentum spectrum or angular distribution. The investigation in this direction should be very challenging and deserves attention in the near future. We would, however, stress, in connection with points (iv) and (v), that the analysis with the help of the present model of a large body of experimental data available at $E_{\text{beam}} = 800$ MeV leaves little room for exotic phenomena [4]).

We would like to thank Dr. S.E. Koonin for his encouragement and for a careful reading of the manuscript. We thank the IISN (Belgium) for financial support. One of us (JC) is very grateful to the members of the Kellogg Radiation Laboratory for their kind hospitality. One of the authors (TM) would like to thank the members of the Service de Physique Théorique, University of Liège, where a large part of this work has been done.

References

1) G.D. Westfall, J. Gosset, P.J. Johansen, A.M. Poskanzer, W.G. Meyer, H.H. Gutbrod, A. Sandoval and R. Stock, Phys. Rev. Lett. **37** (1976) 1202
2) R.L. Hatch and S.E. Koonin, Phys. Lett **81B** (1979) 1
3) J. Cugnon, T. Mizutani and J. Vandermeulen, Nuovo Cim. Lett. **28** (1980) 55
4) J. Cugnon, Phys. Rev. **C**, in press
5) J.P. Bondorf, P.J. Siemens, S. Garpmann and E. Halbert, Z. Phys. **279** (1976) 385
6) J. Hüfner and J. Knoll, Nucl. Phys. **A290** (1977) 460
7) J. Knoll and J. Randrup, Nucl. Phys. **A324** (1979) 445
8) J. Randrup, Nucl. Phys. **A314** (1979) 429
9) A.R. Bodmer and C.N. Panos, Phys. Rev. **C15** (1977) 1342
10) L. Wilets, E.M. Henley, M. Draft and A.D. Mackellar, Nucl. Phys. **A282** (1977) 341
11) D.J.E. Callaway, L. Wilets and Y. Yariv, Nucl. Phys. **A327** (1979) 250
12) I. Montvay and J. Zimányi, Nucl. Phys. **A316** (1979) 490
13) A.A. Amsden, A.S. Goldhaber, F.H. Harlow and J.R. Nix, Phys. Rev. **C17** (1977) 2080
14) A.A. Amsden, F.H. Harlow and J.R. Nix, Phys. Rev. **C15** (1977) 2059

15) H. Stöcker, J.A. Maruhn and W. Greiner, Z. Phys. **A293** (1979) 173
16) Y. Yariv and Z. Fraenkel, Phys. Rev. **C20** (1979) 2227
17) K. Smith and M. Danos, Proc. of the Fall Creek Falls State Park Conference, Tennessee, June 1977, ORNL Conf-770602, p. 363
18) Particle Data Group, NN and ND interactions (above 0.5 GeV/c). A Compilation, UCRL-20000 NN, 1970
19) G.J. Igo, Rev. Mod. Phys. **50** (1978) 523
20) J.N. Ginocchio, Phys. Rev. **C17** (1978) 195
21) E. Ferrari and F. Selleri, Nuov. Cim. **27** No 6 (1963) 1450
22) W.M. Kloet, R.R. Silbar, R. Aaron and R.D. Amado, Phys. Rev. Lett. **39** (1977) 1643
23) M. Hirata, J.H. Koch, F. Lenz and E.J. Moniz, Phys. Lett **70B** (1977) 281
24) E. Oset and W. Weise, Nucl. Phys. **A319** (1979) 477
25) M. Hirata, F. Lenz and Y. Yuzaki, Ann. of Phys. **108** (1977) 116
26) J.P. Bondorf, H.T. Feldmeier, S. Garpmann and E.C. Halbert, Phys. Lett. **65B** (1976) 217
27) R. Hagedorn, Cargèse lectures in Physics, Vol. 6 (Gordon and Breach, NY, 1973)
28) G.F. Bertsch, Phys. Rev. **C15** (1977) 713
29) B. Jakobsson, J.P. Bondorf and G. Tsai, Phys. Lett. **82B** (1979) 35
30) A. Sandoval *et al.*, Proc. Ettore Majorana School on heavy-ion interactions at high energy, Erice 1979, to be published
31) P.J. Siemens and J.O. Rasmussen, Phys. Rev. Lett. **42** (1979) 880
32) S. Nagamiya, Proc. 4th High Energy Heavy Ion Summer Study, Berkeley, 1978, LBL-7766, p. 71
33) G.F. Chapline, M.H. Johnson, E. Teller and M.S. Weiss, Phys. Rev. **D8** (1973) 4302
34) G. Bizard *et al.*, Nucl. Phys. **B108** (1976) 189
35) H.H. Gutbrod, Proc. 4th High Energy Heavy Ion Summer Study, Berkeley, 1978, LBL-7766, p. 1
36) G.F. Bertsch, Phys. Rev. Lett. **34** (1975) 697
37) S.I.A. Garpmann, D. Sperber, N.K. Glendenning and Y. Karant, Phys. Lett. **86B** (1979) 133
38) T.D. Lee and G.C. Wick, Phys. Rev. **D4** (1971) 1601
39) M. Gyulassy and S.K. Kauffmann, Phys. Rev. Lett. **40** (1978) 298
40) A.B. Migdal, JETP (Sov. Phys.) **34** (1972) 1182
41) P. Hecking and H.J. Pirner, Nucl. Phys. **A333** (1980) 514